

MULTIPHASE FLOW LES STUDY OF THE FUEL SPLIT EFFECTS ON COMBUSTION INSTABILITIES IN AN ULTRA LOW-NOX ANNULAR COMBUSTOR

M. Bauerheim *

T. Jaravel

L. Esclapez

CERFACS
42 ave Gaspard Coriolis
31057, Toulouse, France

SNECMA Villaroche
77550 Reau, France
Email: bauerheim@cerfacs.fr

E. Riber

L.Y.M. Gicquel

B. Cuenot

CERFACS
42 ave Gaspard Coriolis
31057, Toulouse, France

M. Cazalens

S. Bourgois

M. Rullaud

SAFRAN TECH
77550 Moissy-Cramayel, France

SNECMA Villaroche
77550 Reau, France

ABSTRACT

This paper describes the application of a coupled Acoustic model/LES approach to assess the effect of fuel split on combustion instabilities in an industrial ultra low-NOx annular combustor. Multiphase flow LES and an analytical model (ATACA-MAC) to predict thermoacoustic modes are combined to reveal and compare two mechanisms leading to thermoacoustic instabilities: 1) a gaseous type in the multi-point zone where acoustics generates vortex shedding, wrinkling the flame front and 2) a multiphase flow type in the pilot zone where acoustics can modify the liquid fuel transport and the evaporation process leading to gaseous fuel oscillations. The aim of this paper is to investigate these mechanisms by changing the fuel split (from 5% to 20%, mainly affecting the pilot zone and mechanism 2) and therefore assess which mechanism controls the flame dynamics. First, the eigenmodes of the annular chamber are investigated using the analytical model and validated by 3D Helmholtz simulations. Then, multiphase flow LES are forced at the eigenfrequencies of the chamber for three different fuel split values. Key features of the flow and flame dynamics are investigated. Results show that acoustic forcing generates gaseous fuel oscillations which strongly depend on the fuel split parameter. However, the global

correlation between heat release fluctuations and acoustics highlights no dependency on the fuel split staging. It suggests that vortex shedding in the multi-point zone, almost not depending on the fuel split here, is the main feature controlling the flame dynamics for this LEMCOTEC engine.

NOMENCLATURE

α	Fuel split
n	Gain of the FTF
τ	Time-delay of the FTF
ρ	Density
u	Axial velocity
p	Pressure
q	Heat release
φ	Equivalence ratio
$\hat{\varphi}$	Equivalence ratio fluctuations
$\hat{\omega}$	Vorticity fluctuations
\hat{q}	Heat release fluctuations
ω	Angular frequency
f	Frequency (normalized)
$\Delta\phi$	Phase lag between fuel oscillations and acoustics
$\Delta\phi_V$	Phase lag between vortex shedding and acoustics

*Address all correspondence to this author.

$\Delta\phi_Q$ Phase lag between global heat release and acoustics
 N Number of burners

FTF Flame Transfer Function

$AVSP$ Helmholtz solver

$AVBP$ Compressible multiphase flow LES solver

$LADTF$ Locally Adaptative Dynamic Thickened Flame model

$ATACAMAC$ Analytical tool to analyze azimuthal modes

$-$ Mean quantity

$/$ Fluctuating quantity

$\hat{\cdot}$ Fourier transform

INTRODUCTION

Moving toward very high OPR engines to reduce pollutant emissions requires to push the lean burn technologies towards their limits. Inherent drawbacks of these new technologies have to be accounted for at the design stage. This observation is especially true when innovative lean combustion chambers with multi-point injection systems are used since they are prone to combustion instabilities, a phenomenon investigated here in the LEMCOTEC¹ engine. These thermo-acoustic instabilities correspond to the coupling between acoustics and the unsteady heat-release. This interaction usually involves intermediate convective mechanisms such as vortex shedding [1] or fuel oscillations [2]: they are still partially unknown and therefore constitute the main topic of this paper. Under some conditions, this coupling can become unstable giving rise to strong pressure oscillations in the chamber, which can affect significantly the engine performance or even damage the combustion chamber [3].

Predicting such unstable acoustic modes appearing in annular gas turbines has been the topic of multiple research activities over the last decade [3–7]. To tackle the complexity of this problem, numerical methods have progressed in three directions as shown in Fig. 1: (1) Analytical and low-order models have been developed [6, 8, 9] to reduce computational costs and provide clues on the underlying phenomena involved in combustion instabilities, (2) 3D acoustic tools [10, 10, 11] have been used to predict unstable modes in complex industrial combustors and (3) LES of isolated sectors or full 360° annular chambers have been performed [12].

Today, all these tools have to be used together to identify unstable modes and assess the sensitivity of the growth rate to uncertain parameters (geometric details, operating points etc.) or models (turbulence, boundary conditions etc.) [14]. These methodologies are applied in this paper on the liquid-fueled annular chamber LEMCOTEC. In particular, two intermediate mechanisms controlling thermoacoustic oscillations are investigated: (1) a classical gaseous type where acoustics (\hat{p}) generates

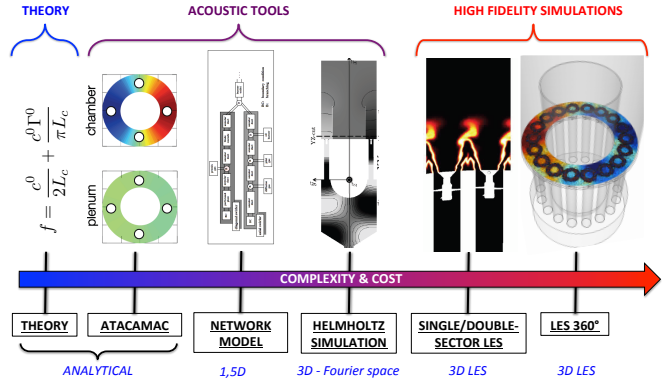


FIGURE 1: Tools developed at CERFACS for combustion instabilities: low-order models (ATACAMAC), Helmholtz simulations (AVSP) and large eddy simulations (AVBP) [13]

a vortex shedding (i.e. unsteady vorticity $\hat{\omega}$) which propagates downstream and interacts with the flame [1] (Fig. 2, top) and (2) a multiphase type where acoustics can modify the liquid fuel transport, its evaporation generating gaseous fuel oscillations [2] ($\hat{\phi}$, Fig. 2, bottom). The global heat release fluctuations \hat{q} can therefore be modeled by [15]:

$$\frac{\hat{q}}{\bar{q}} = \underbrace{\hat{p}/\bar{p}}_{\text{Negligible}} + \underbrace{\text{FTF}_p(\omega)\frac{\hat{p}}{\bar{p}}}_{\text{Vortex shedding}} + \underbrace{\text{FTF}_\phi(\omega)\frac{\hat{\phi}}{\bar{\phi}}}_{\text{Fuel oscillations}} \quad (1)$$

where FTF_p is the flame response to the vortex shedding induced by acoustics (\hat{p} or \hat{u}) and wrinkling the flame surface, FTF_ϕ is the flame response to the equivalence ratio fluctuations $\hat{\phi}$, and \bar{a} and \hat{a} correspond to the mean and Fourier transform of any variable a . The relative density fluctuation \hat{p}/\bar{p} is neglected here since $\hat{p}/\bar{p} = \hat{p}/\bar{p} \ll 1$ (small acoustic disturbances assumption).

In industrial configurations equipped with multi-point injection systems, these two mechanisms (Fig. 2) can appear simultaneously. Consequently, the question of which mechanism is driving the instability is of crucial importance to stabilize the unstable modes. This issue becomes even more complex in combustion chambers where fuel is injected at several locations, generating multiple flames: some flames can exhibit the first mechanism while the others can be affected by the second mechanism, or even a combination of them. For example, in a configuration with two flames, where vortex shedding controls “Flame 1” and fuel oscillations control “Flame 2”, Eq. (1) becomes in a simple form:

$$\frac{\hat{q}}{\bar{q}} = \underbrace{\alpha \text{FTF}_p(\omega)\frac{\hat{p}_1}{\bar{p}}}_{\text{Flame 1}} + \underbrace{(1-\alpha) \text{FTF}_\phi(\omega)\frac{\hat{\phi}_2}{\bar{\phi}}}_{\text{Flame 2}} \quad (2)$$

¹Low EMissions COre-engine TEChnologies.

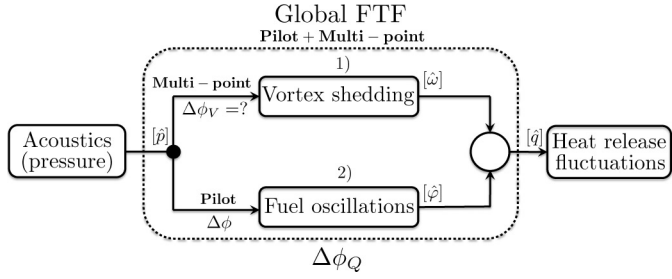


FIGURE 2: Block diagram showing that acoustics affects both Mechanism 1 (vortex shedding $\hat{\omega}$) and 2 (fuel oscillations $\hat{\varphi}$), leading to heat release oscillations \hat{q} . In this paper, LES allows the identification of these mechanisms and shows that Mechanism 1 occurs at the multi-point zone and Mechanism 2 at the pilot zone.

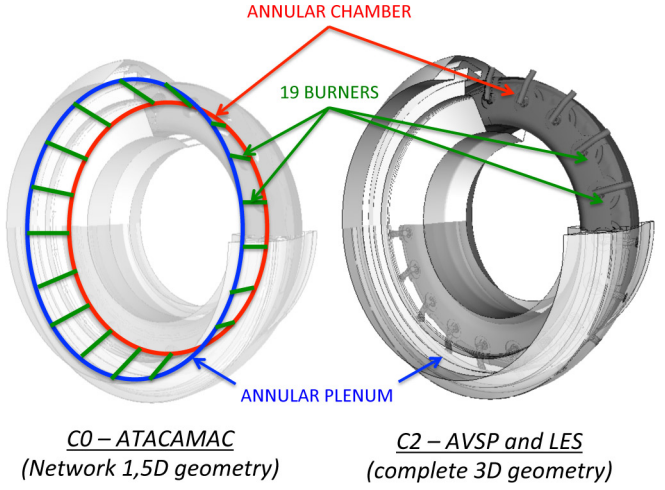


FIGURE 3: The ultra low-NOx annular configuration LEMCOTEC with $N = 19$ identical sectors. Network model for ATACAMAC (C0 - left) and a complete configuration with detailed swirlers for Helmholtz simulations and LES (C2 - right).

THE ULTRA LOW-NO_X ANNULAR CONFIGURATION LEMCOTEC

The target configuration is the ultra low NO_x combustor currently developed by SNECMA as part of the LEMCOTEC project (Fig. 3, right). Each of the $N = 19$ identical sectors (Fig. 4) comprises a flame tube, an inner as well as an outer bypass lines, and a multi-point injection system to achieve low emission targets while keeping operability for the whole power range. This type of injection system is designed to generate two distinct flames:

- (i) The pilot zone (PZ) is controlled with a central fuel injector and an axial swirler. The resulting central pilot flame burns near stoichiometric conditions. The high temperature of the recirculating flow is a strong stabilization mechanism at low-power conditions.
- (ii) The multi-point zone (MPZ) is controlled with a radial swirler and a multipoint injector (multiple holes in the inner part of the swirler). Injection of fuel in this swirling environment promotes efficient atomization and rapid mixing between liquid fuel and air. The fuel-air ratio in this zone is chosen to obtain lean conditions. The multi-point flame provides most of the power at high-power conditions such as take-off and cruise. Lean burn and associated low flame temperature is indeed essential to accomplish low emission levels.

Gaseous air from the compressor is injected at the diffuser exit and enters the annular plenum as well as the swirler with a high temperature and pressure (typically around several MPa), corresponding to the take-off operating point retained in this

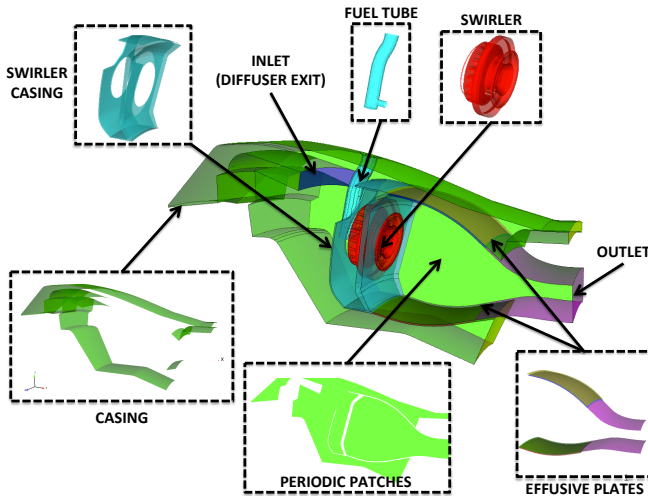


FIGURE 4: Single sector of the industrial ultra low-NOx configuration LEMCOTEC.

study as a high-power regime especially prone to instabilities. Liquid fuel is injected in both the pilot and multi-point zones and mixes with air after evaporation. The fuel split parameter α , defined as the ratio between the mass flow rate in the pilot zone and the total fuel mass flow rate, is varied from 5% to 20% (i.e., mainly affecting the pilot injection), the reference case being $\alpha = 10\%$. The global equivalence ratio is $\varphi = 0.42$, leading to a lean combustion regime. The corresponding laminar flame thickness is $\delta_f^0 \approx 45\mu\text{m}$, which implies improvements of the standard thickened flame methodology. A new methodology is therefore proposed in this paper to tackle this issue.

EIGENMODES OF THE ANNULAR COMBUSTOR

Prior to a complete stability analysis, the forcing angular frequencies ω , used to excite mechanisms 1 and 2 (Fig. 2) in the LES, have to be determined. Two different strategies have been developed recently to analyze azimuthal modes in 360° configurations: (1) 3D Helmholtz solvers, like AVSP [17] used in this study, have been adapted to annular chambers [10, 10, 11] and (2) analytical approaches, such as ATACAMAC [8, 18] used here, have been proposed to avoid the costs of 3D formulations. This last class of approach is especially interesting to elucidate mechanisms, such as transverse forcing effect [9], symmetry breaking [6] and mode nature [19–21], since they can provide explicit solutions for the frequency and the growth rate of all modes. These two methods are used and compared here to investigate first (1) the eigenmodes of the LEMCOTEC engine with $N = 19$ burners and passive flames (no acoustics/flame coupling) and then (2) to anticipate the acoustic/flame coupling effect on the eigenfrequencies (active flames modeled by FTFs).

Acoustic modes with passive flames

First, ATACAMAC and AVSP are used with passive flames to provide a first clue on forcing frequencies. Analytical approaches can predict unstable modes in simplified configurations while retaining most of the important physical phenomena and geometrical specificities of industrial annular chambers. ATACAMAC (Analytical Tool to Analyze and Control Azimuthal Modes in Annular Chambers), developed at CERFACS [8, 18], is based on a quasi one-dimensional network modeling the annular plenum and the annular chamber connected by N burners (Fig. 3, left). The chamber outlet corresponds to a choked nozzle, approximated by an acoustic boundary condition $u' = 0$. However, no data is available for the plenum inlet. For the sake of simplicity, a condition $u' = 0$ was also used for the plenum inlet.

Three different types of output are provided by ATACAMAC (1) under a small perturbation assumption, fully analytical expressions of the frequency and growth rate of azimuthal modes are derived depending on the FTFs (null for passive flame computations), (2) a numerical approximation of the frequencies and growth rates without consideration on the perturbation level and (3) the mode structure in the annular cavities to highlight coupling mechanisms between the annular plenum and the annular chamber [18].

ATACAMAC results² for the first three azimuthal modes are displayed in Fig. 5 and are compared with Helmholtz results obtained by AVSP (Fig. 6). AVSP is a 3D code devoted to the resolution of acoustic modes of complex industrial combustors [17]. It solves the eigenvalue problem obtained by discretizing the Helmholtz equation. Compared to ATACAMAC, all geometric details can be retained and more realistic baseline flow fields for density and sound speed can be extracted from LES. AVSP is capable of predicting not only azimuthal modes but also longitudinal or even radial or mixed modes. Both frequencies and mode structures predictions given by ATACAMAC (f) and AVSP (f^*) are in good agreement and can be identified:

- (i) Mode at $f = 1.007$ ($f^* = 1.0$) is the first azimuthal mode associated to the plenum geometry. Both tools show that acoustic activity is present in the annular chamber as well (50% of the pressure level in the plenum).
- (ii) A longitudinal mode at $f^* = 1.429$ is obtained by AVSP but not ATACAMAC since only azimuthal modes are thought for.
- (iii) Mode at $f = 1.800$ ($f^* = 1.847$) is the second azimuthal mode associated to the plenum. No acoustic is observed in the chamber.
- (iv) Mode at $f = 1.799$ ($f^* = 1.83$) is the first azimuthal mode of the chamber. Note that such results show that simple analytical tools are able to separate and identify close acoustic modes ($f^* = 1.79$ and $f^* = 1.80$).

²Frequencies and growth rates have been normalized by the output of the Helmholtz solver AVSP corresponding to the first azimuthal mode.

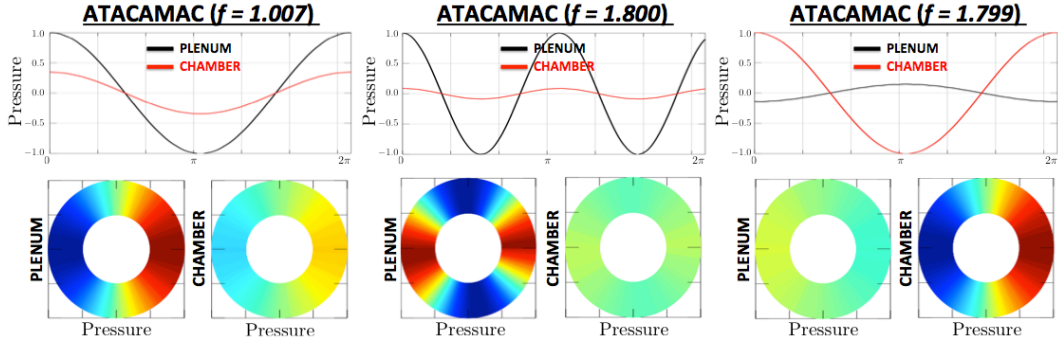


FIGURE 5: ATACAMAC results of the three first azimuthal modes of the LEMCOTEC configuration with $N = 19$ burners and passive flames: normalized frequency (top), pressure plots over the azimuthal direction (middle) and pressure fields in annular cavities (bottom).

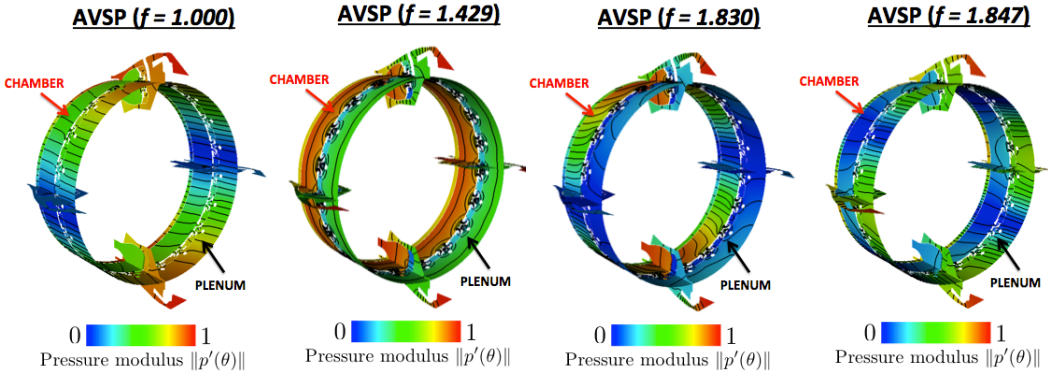


FIGURE 6: AVSP results of the first three azimuthal modes ($f = 1.0, 1.830$ and 1.847) and one longitudinal mode ($f = 1.429$) of the annular LEMCOTEC configuration with passive flame.

Analytical acoustic modes with active flames

The ATACAMAC tool has been validated against 3D Helmholtz simulations and a very good agreement is found for passive flames. However, Bauerheim et al. [18] have shown that incorporating delayed processes, as the ones presented in Fig. 2, can modify both the coupling between annular plenum and chamber (and so eigenfrequencies at which forcing has to be performed) and hereby the stability analysis. Figure 7 displays the frequencies and growth rates depending on the input Flame Transfer Function, which links the acoustics pressure \hat{p} to the unsteady heat release \hat{q} : $FTF_p = \frac{\hat{q}p_0}{\hat{p}q_0} = n_p e^{j\Delta\phi_Q}$. Note that using a correlation with the acoustic pressure \hat{p} or the axial velocity \hat{u} leads to equivalent results in the harmonic regime, since they are related by the impedance $Z(\omega) = \hat{p}/(\rho^0 c^0 \hat{u})$.

ATACAMAC results (Fig. 7) show that the azimuthal modes of the LEMCOTEC engine are “weakly coupled”, i.e. eigenfrequencies are not strongly modified by the flame/acoustic interactions: $f^* = 1.0, 1.43$ and 1.84 can be used as forcing frequencies in the LES. Moreover, for weakly coupled modes, stability is

given by [18]:

$$Im(\omega) \propto n_u(\alpha)N \sqrt{\frac{\gamma_b T_u^0}{\gamma_u T_b^0}} \sin(\Delta\phi_u(\alpha)) \quad (3)$$

where $Im(\omega)$ is the growth rate of the azimuthal mode, N is the number of burners designed to comply with light-around constraints [22] while T^0 and γ are the temperature and the ratio of the constant volume and constant pressure heat capacities in the unburnt (u) and burnt (b) gases depending on the operating condition of the engine. n_u and $\Delta\phi_u$ are the amplitude and phase-lag of the classical FTF describing the interaction between the unsteady combustion and the acoustic velocity ($FTF_u = \frac{q' u_0}{u' q_0} = n_u e^{j\Delta\phi_u}$), linked to FTF_p previously described³. Therefore, the stability depends only here, at first order and without taking into account losses, on the phase-lag $\Delta\phi_u(\alpha)$, other parameters being always positive. This paper intends to investigate multiphase flow mechanisms encountered in the LEMCOTEC engine equipped with a

³ $FTF_u = \frac{q' u_0}{u' q_0} = \frac{q' p_0}{p' q_0} \times \frac{p' u_0}{u' p_0} = \frac{q' p_0}{p' q_0} \times \frac{p'}{\rho^0 c^0 u'} \times \frac{\rho^0 c^0 u^0}{p^0} = FTF_p \times Z(\omega) \times \gamma M$

multi-point injection system which lead to such a phase-lag and evaluate its dependency with the fuel split α .

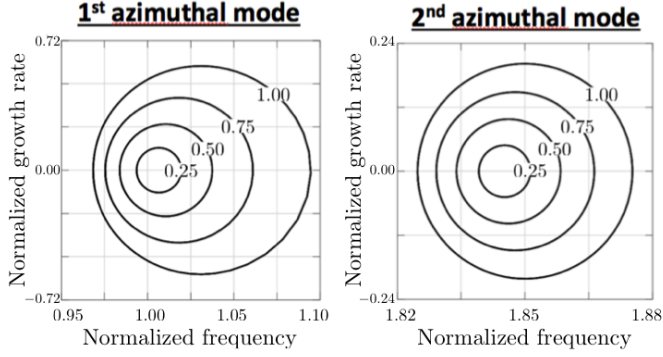


FIGURE 7: Stability maps obtained by ATACAMAC for the first and second azimuthal modes of the annular engine vs. varying FTF_u amplitudes ($n_u = 0.25$ to 1.0) and phase-lags ($\Delta\phi_u = 0$ to 2π).

LARGE EDDY SIMULATION

LES is widely recognized as an accurate method [23] to study ignition [24], temperature profiles at the combustor exit and combustion instabilities [12, 25] in complex configurations. Coupled to analytical tools, LES results can provide essential clues on the underlying phenomena driving combustion instabilities. In this paper, delayed liquid/gaseous mechanisms leading to combustion instabilities are searched for according to analytical results provided by ATACAMAC (Eq. (3)).

Mesh and numerical setup

Multiphase flow LES presented hereafter are obtained using the AVBP solver on a single sector of the annular combustor with periodic boundary conditions in the azimuthal direction. Filtered fully compressible multispecies Navier-Stokes equations are solved on an unstructured grid containing 28 millions cells, corresponding to a characteristic length of 0.35mm in the flame region (Fig. 8). A centered spatial scheme with explicit time-advancement of 3rd order in both space and time is used [26]. Turbulent subgrid stresses are modeled with the WALE approach [27]. The air inlet and combustor outlet are described by Navier-Stokes Characteristic Boundary Conditions (NSCBC) [28] to ensure proper treatment of acoustic wave propagation as well as reflection. Walls are considered no-slip and adiabatic.

The liquid phase (kerosene) is modeled using an Eulerian approach with the assumption of a locally mono-disperse liquid

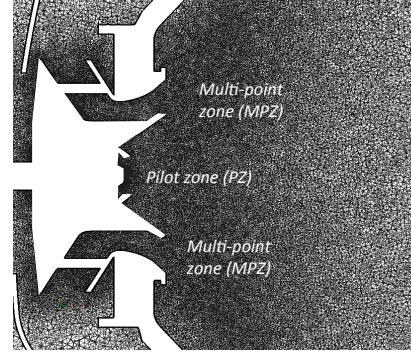


FIGURE 8: Mesh around the swirler, pilot and multi-point zones. Details of the swirler and injection system have been blanked.

phase. This methodology, implemented in AVBP, has been intensively validated [29]. First, this Eulerian approach has been compared with a Lagrangian approach and experimental [30] data on a liquid jet in-crossflow configuration. More complex validation cases have been also performed, for example on the TLC configuration containing a multi-point injection system, similar to the one studied here. Comparisons between Eulerian [29, 31] and Lagrangian [29, 32] approaches with experimental data show a very good agreement. Recently, Eulerian approach has been applied to simulate the complete ignition sequence of a liquid-fueled gas turbine [33]. Similar validations (Eulerian vs. Lagrangian approaches, isolated sector vs. 360° configuration etc.) are currently conducted at CERFACS with AVBP on the LEM-COTEC engine, regarding ignition sequences and temperature profiles (FRT) issues [22].

In this study, several fuel split ($\alpha = \frac{\dot{m}_{PZ}}{\dot{m}_{PZ} + \dot{m}_{MPZ}}$) are tested to assess its impact on flame dynamics and phase-lag $\Delta\phi$ (Fig. 2): $\alpha = 5\%$, 10% and 20%. The FIMUR methodology [34] is used to model the fuel spray generated by the atomizer. However, no LES model is incorporated to take into account the interaction between acoustics and atomization. Consequently, this study only considers the effects of acoustics on evaporation and transport for the liquid phase. Chemistry is described by a 6 species, 2-step reduced mechanism with pre-exponential adjustments to correctly reproduce flame speed and temperature for kerosene-air combustion over the whole range of flammability. The artificially Dynamic Thickened Flame model (DTF) is used [35] to resolve the flame on the LES grid and to account for turbulence/chemistry interactions. Nevertheless, as displayed in Fig. 9, the flame structure is complex with a pilot and a multi-point zones, which can burn in both premixed and non-premixed regimes⁴. Thus, due to the high pressure (a few MPa) and the large range of flammability and fuel stratification (typically, the equivalence ratio φ varies from 0 to 2.0, Fig. 9), improvement of

⁴Non-premixed flames are localized where heat release (thin black lines) iso-contours follow the stoichiometric lines (large blue lines)

the standard DTF model is required to avoid too large thickening factors or too fine meshes.

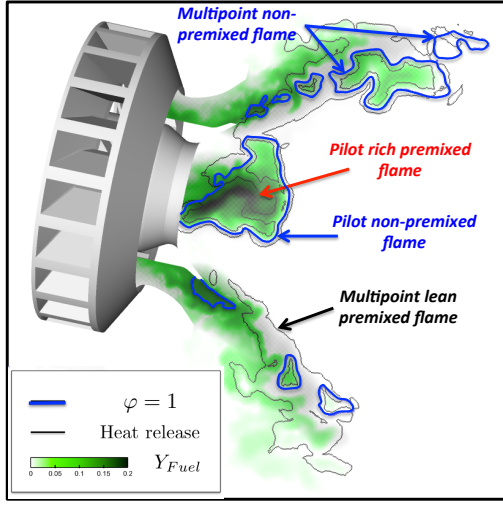


FIGURE 9: Instantaneous flame nature (premixed or non-premixed), for the case $\alpha = 10\%$, identified using the fuel mass fraction field and iso-contours of heat release (thin black lines) and the stoichiometric lines ($\varphi = 1$, large blue lines).

Locally adaptative dynamic thickened flame model

In complex industrial gas turbines operating at high pressure, the resolution of the flame of typical thickness $\delta_f^0 \sim 10 - 100 \mu m$ would lead to very fine meshes out-of-reach today. Colin et al. [26] have proposed a method to artificially thicken the flame allowing its resolution on standard meshes: the thickened flame thickness is $\delta_f^1 = \mathcal{F} \delta_f^0$, where \mathcal{F} is called the thickening factor. In the Dynamics Thickened Flame (DTF) model, the thickening is applied only on the flame zone ($\mathcal{F} = 1 + (\mathcal{F}_{max} - 1)\mathcal{S}$), the reactive zone being detected by a sensor \mathcal{S} . An efficiency function \mathcal{E} [35] is introduced to recover the correct flame response to turbulence:

$$\mathcal{S} = \tanh\left(\beta \frac{\Omega}{\Omega_0}\right), \quad \mathcal{E} = \frac{\Xi(\delta_f^1, s_f^0)}{\Xi(\delta_f^0, s_f^0)} \quad (4)$$

where β is a parameter defined manually (a typical value is 50), Ω is the heat release, Ω_0 a heat release threshold and s_f^0 is the laminar flame speed.

This methodology works well for premixed combustors but complications appear in non-premixed chambers where the equivalence ratio φ varies locally (typically from 0 to 2.0), leading to high thickening factors beyond the limits of validity of this

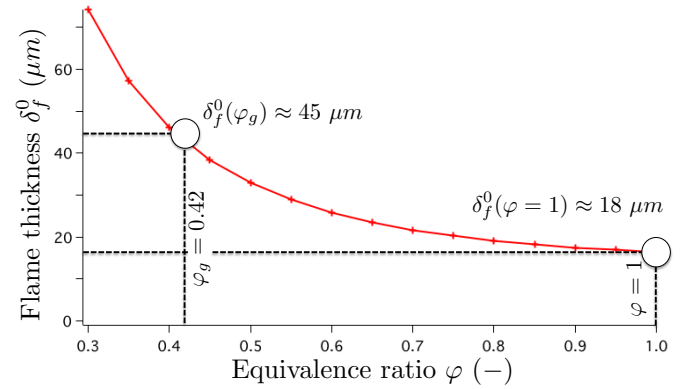


FIGURE 10: Laminar flame thickness variations with the local equivalence ratio φ . The flame thickness is minimum near stoichiometric conditions $\varphi = 1$.

methodology. Parameters defining the thickening factor (Ω_0) and the efficiency function (δ_f^0 and s_f^0) also vary with the local equivalence ratio (Fig. 10). However, these parameters are usually kept constant, based on the stoichiometric condition ($\delta_f^0(\varphi = 1)$), even in lean regions where the effective flame thickness is higher, requiring smaller thickening factors. Configurations using multipoint injection systems, designed to operate near stoichiometry in the pilot zone but in a lean regime in multi-point zones, are particularly prone to this issue. Consequently, a Locally Adaptive Dynamic Thickened Flame mode (LADTF) is developed:

- (i) Using Cantera, a collection of laminar flames at various equivalence ratios φ are computed and parameters δ_f^0 , s_f^0 , and Ω^0 are tabulated vs. the equivalence ratio.
- (ii) During the computation, $\varphi(\vec{x})$ is computed locally and tables $\delta_f^0(\varphi)$, $s_f^0(\varphi)$, and $\Omega^0(\varphi)$ are interpolated to compute a local thickening factor $\mathcal{F}_{loc}(\vec{x})$ and associated efficiency function $\mathcal{E}_{loc}(\vec{x})$.

For the LEMCOTEC engine, this approach allows an effective reduction of the applied thickening factors, going from 70 to 28 in lean regions.

FLAME SHAPE AND DYNAMICS

ATACAMAC and AVSP have been applied to the LEMCOTEC engine (Figs. 5 and 6) to provide eigenfrequencies of the system. From a stable computation [22], an acoustic wave at the eigenfrequencies found by AVSP/ATACAMAC is injected at the outlet into the computational domain using the NSCBC methodology [28]. This wave propagates upstream and interacts with the flame before leaving the computational domain at the inlet (non-reflecting boundary conditions are therefore required). Since the ATACAMAC results have shown that modes of the

configuration are “weakly coupled” [18], the stability of the configuration can be studied by investigating phase lags between the unsteady combustion and acoustics. The global unsteady heat release $q'(t)$, or fuel oscillations $Y'_{kero}(t)$, will be recorded and correlated to the axial velocity fluctuations $u'(t)$ or pressure $p'(t)$ giving access to these phase-lags. Since the harmonic regime is considered here, the acoustic velocity and pressure are linked by the impedance, which depends only on the angular frequency ω : $Z(\omega) = p' / (\rho^0 c^0 u')$. Consequently, except at specific locations like pressure or velocity nodes, a correlation with u' or p' leads to equivalent results on the effect of fuel split on the phase-lags. The forcing is axial and performed on a single sector since the azimuthal mode in the annular plenum or annular chamber acts like a clock imposing an axial fluctuating mass flow rate in the burners [36]. This methodology avoids heavy 360° LES computations by separating the two “worlds”: (1) the “acoustic world” where cheaper Helmholtz solvers or analytical tools can be used to retrieve the azimuthal mode frequency as well as structure and (2) the “convective world” addressed by LES, where the flame/acoustics interaction, controlled by convection phenomena (vortex shedding due to acoustics, fuel transport etc.), can be extracted.

Unsteady combustion in a multi-point industrial combustor

The three frequencies obtained by ATACAMAC and AVSP ($f^* = 1.0, 1.43$, and 1.83) for the three fuel splits ($\alpha = 5\%$, 10% , and 20%) have been computed with an acoustic pressure level $p'/p_{mean} = 0.5\%$ to be consistent with the linear framework assumption. Fuel split is modified by changing the pilot axial injection velocity $u_0 = u_0(\alpha)$. First, unsteady combustion mechanisms of a multiphase flow LES containing a pilot and multi-point flames have to be identified. Note that no precessing vortex (PVC) is observed in both the unforced and the forced cases. The flame dynamics under acoustic forcing is examined using Dynamic Mode Decomposition (DMD), which provides the modulus $\|T'_{DMD}\|$ and the phase ϕ_{DMD} of the temperature oscillations $T'_{DMD} = \|T'_{DMD}\| \cos \phi_{DMD}$ (this fluctuating temperature is normalized in Fig. 11). The phase information is associated to the nature of the oscillations: if $\phi_{DMD} = \phi_0 + k\pi$, $k \in \mathbb{N}$ (i.e. constant with jumps equal to π), then the fluctuation is standing; if $\phi_{DMD} = \lambda x_s$ (i.e. linear phase with the spatial coordinate x_s), then the fluctuation is propagating. Figure 11 displays the temperature fluctuations obtained by DMD (top) as well as the phase ϕ_{DMD} (bottom) along two characteristic paths: the path (1) in the pilot zone and the path (2) in the multi-point zone. The results show that:

- (i) The pilot zone exhibits weak standing oscillations (constant phase), characteristic of a flapping phenomenon (Fig. 11, ---, left).
- (ii) Strong propagating fluctuations (linear phase) occur in the

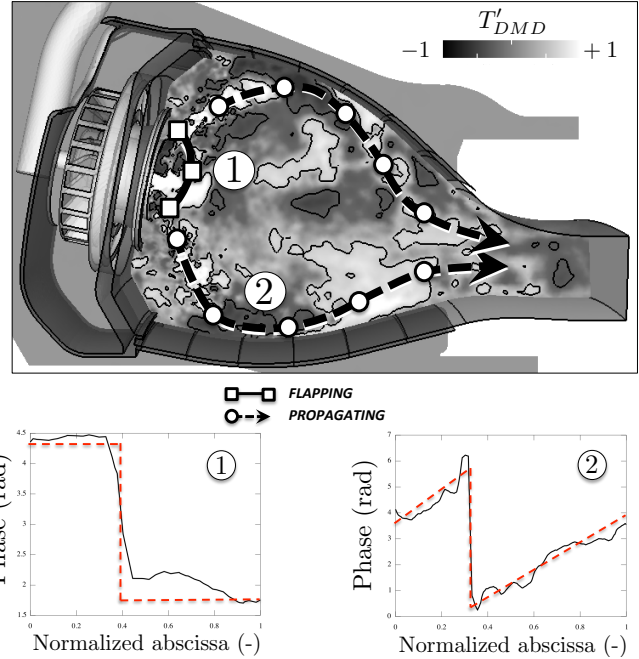


FIGURE 11: Temperature fluctuations obtained by DMD for the case $f = 1.84$ and $\alpha = 10\%$. Two different behaviors are identified using the phase information provided by the DMD and by following the two paths (1) and (2): (1) a standing oscillation associated to flapping (constant phase, bottom) and (2) a propagating fluctuation corresponding to hot spots shedding (linear phase, bottom).

multi-point zone due to hot spots shedding (Fig. 11, ---, right).

These results unveil that pilot and multi-point flames react differently to acoustics. Increasing the fuel split corresponds to increasing the liquid fuel mass flow rate in the pilot zone, resulting in a longer fuel jet which enhances the flapping motion and potentially modifies the stability of the system. Figure 12 displays the instantaneous flame shapes for different fuel splits. The multi-point fuel injection is weakly affected by the fuel split, whereas the pilot fuel injection is drastically modified: the iso-contour of rich fuel mass fractions $Y_{kero} = 0.1$ is five times longer when $\alpha = 20\%$ compared with $\alpha = 5\%$. It results that at all frequencies, the flapping motion disappears at low fuel split ($\alpha = 5\%$), but becomes intense at higher fuel split ($\alpha = 10\%$ or 20%).

Finally, Fig. 13 shows the two mean flame locations (multi-point and pilot) to be compared with the instantaneous Q-criterion indicating vortices (left) and gaseous fuel fluctuations (RMS values, right). It clearly proves that the multi-point flame is mainly affected by small vortices whereas the pilot flame is only affected by strong kerosene fluctuations. This result illus-

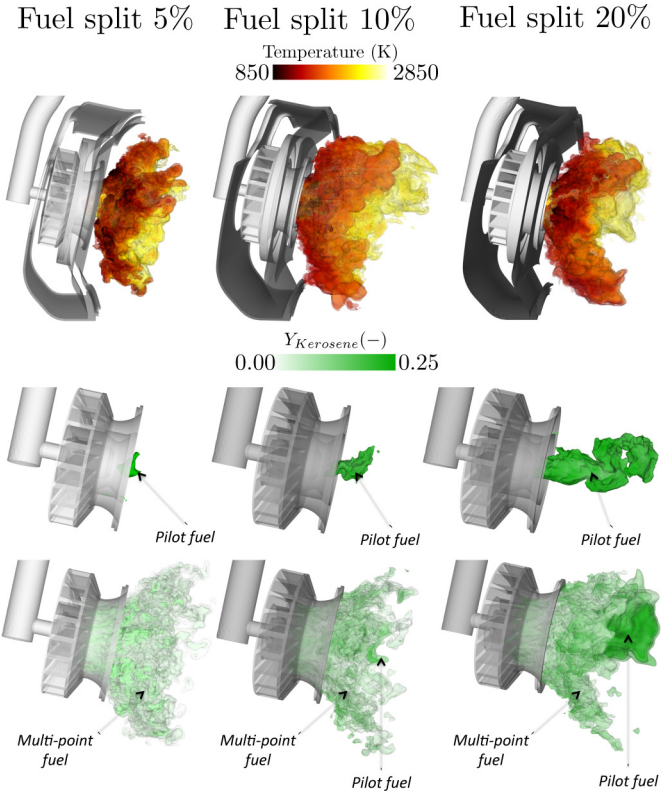


FIGURE 12: Iso-contours of heat release colored by temperature (top), iso-contour of fuel mass fraction (rich, middle) and (lean+reach, bottom) to visualize the flame shape as well as the pilot (middle) and multi-point (bottom) flames vs. the fuel split parameter: 5% (left), 10% (middle) and 20% (right).

trates the two mechanisms retained for this study, as mentioned in Fig. 2, and detailed in the next sections:

- (1) The multi-point flame is wrinkled by vortices ($\hat{\omega}$) induced by acoustic waves (\hat{p}) interacting with the swirler.
- (2) The pilot flame is affected by gaseous fuel oscillations, which modify the local equivalence ratio ($\hat{\phi}$) and then the heat-release (\hat{q}).

Pilot flame: flapping & gaseous fuel oscillations

The flapping oscillations observed in the pilot zone result from the interaction between acoustics and the liquid/gaseous fuel transport as well as evaporation that are crucial phenomena in multiphase flows. This flapping is displayed in Fig. 14, showing the motion of the gaseous pilot fuel jet for the forced case at $f^* = 1.0$ and $\alpha = 20\%$ (iso-surfaces, left ; center lines⁵, right).

⁵ $Y'_{kero}(x, y, z, t)$ = cste corresponds to an iso-surface in the 3D space. For each time $t = t_0$ and longitudinal location $x = x_0$, the iso-surface is averaged in the transverse direction (y, z). It gives the “center lines” of the iso-surface along the

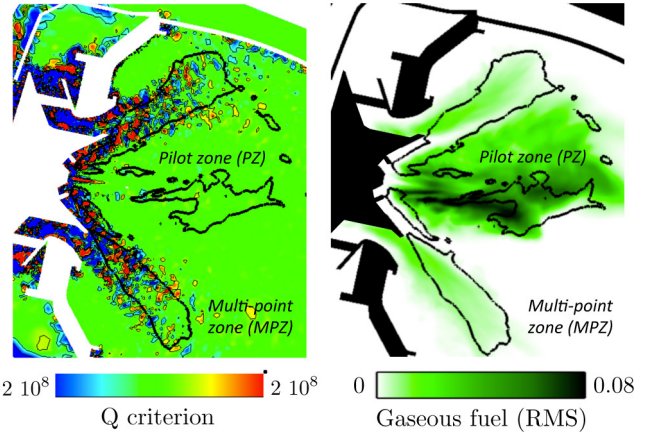


FIGURE 13: Q-criterion (left) and Gaseous fuel oscillations (RMS values, right) in the longitudinal cut-plane. Both the multi-point and pilot mean flames (iso-contour of the mean heat release) are superimposed in solid black lines.

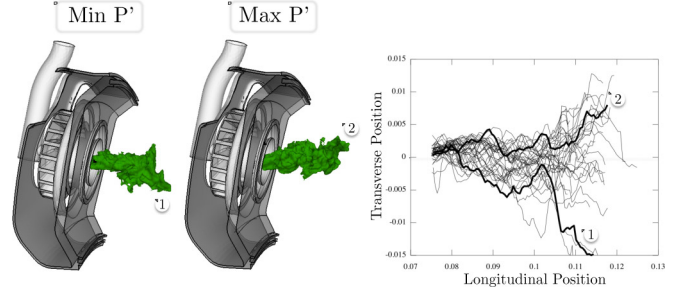


FIGURE 14: Instantaneous iso-surfaces of gaseous fuel corresponding to a minimum (left) and maximum (middle) pressure fluctuations for the case $\alpha = 20\%$ forced at $f^* = 1.0$. The “center line” of 35 similar iso-surfaces (right) are displayed showing a large transverse oscillations of the pilot fuel. “Center lines” of the two cases (1-left and 2-right) are highlighted in bold.

The fuel iso-contours observed in Fig. 14 correspond to gaseous fuel evaporated from the pilot zone, which can then mix with air and burn in the flame front. Acoustic forcing acts on both the fuel transport ($u_0(\alpha) + u'$) and the evaporation taking place upstream of the flame front. Jangi et al. [37] show that two different regimes exist: (1) a synchronous response with the main flow oscillation (quasi-steady condition, low Strouhal number) and (2) a highly unsteady asynchronous mode (high Strouhal number). Acoustic and fuel oscillations in the pilot zone are displayed in Fig. 15, showing that a synchronous mode occurs for the whole frequency range considered here. The fuel oscillations are characterized by the normalized quantity $\widetilde{Y'_{kero}} = Y'_{kero} / p'_{max}$ where

x -direction at each time t (Fig. 14, left).

Y'_{kero} is the fluctuation of the mass fraction of gaseous kerosene and n' is the amplitude of the pressure oscillations. Figures 15

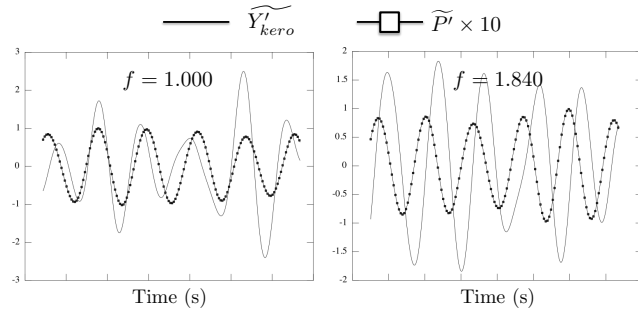


FIGURE 15: Normalized relative pressure $\tilde{P}' = p'/p'_{max}$ and fuel mass fraction $\tilde{Y}'_{kero} = Y'_{kero}/p'_{max}$ oscillations in the pilot zone for the case at $\alpha = 10\%$ and forcing frequencies $f = 1.0$ (left) and $f = 1.84$ (right). A filter at the forcing frequency is applied to remove hydrodynamic and turbulent oscillations.

and 16 also reveal that phase-lags between acoustics and fuel oscillations depend on both the forcing frequency f and the fuel staging α :

- At low forcing frequency ($f = 1.0$, Fig. 15, left), the pressure and kerosene fluctuations are synchronous and in-phase. However, at higher forcing frequencies ($f = 1.84$, Fig. 15, right) pressure and fuel mass fraction oscillations are in quadrature. The resulting relative fuel oscillation is one order of magnitude larger than the forcing pressure amplitude for both cases.
- At constant forcing amplitude, Fig. 16 shows that modifying the fuel split parameter drastically changes the liquid fuel transport or the evaporation process, characterized by its intensity $I_{vap} = \frac{\tilde{Y}'_{kero}}{\tilde{P}'}$ and its normalized phase-lag $\Delta\phi/2\pi$:

$$\tilde{Y}'_{kero} = I_{vap} \tilde{P}'(t - \Delta\phi/\omega) \quad (5)$$

Using low fuel split (e.g. $\alpha = 5\%$) leads therefore to an in-phase fuel oscillations ($\Delta\phi/2\pi \ll 1/4$) while for higher fuel splits ($\alpha = 10\%$ and 20%), oscillations of fuel and pressure are in quadrature phase ($\Delta\phi/2\pi \approx 1/4$). The intensity I_{vap} is almost constant ($I_{vap} \approx 12 - 15$) for all cases.

Multi-point flame: vortex and hot spots shedding

The pilot flame has been investigated and found to change drastically with the fuel split. However, even if Fig. 12 highlights only minor changes in the multi-point flame, it carries most

of the power of the engine and therefore a small variation with the fuel split can generate a significant modification of stability. As shown by DMD, the multi-point zone is controlled by hot spots shedding (Fig.11) due to vortex interacting with the flame (Fig. 13). However, extracting vorticity waves and computing phase-lags between this phenomenon and acoustics remain a complex task. To workaround this issue, the global phase-lag between the whole unsteady heat release $\Delta\phi_Q$ (pilot+multi-point) is extracted and compared with $\Delta\phi$ (Fig. 2).

The idea is that the global Flame Transfer Function (FTF) is the combination of the pilot and multi-point mechanism, as mentioned in Eq. (2):

$$\Delta\phi_Q = f(\Delta\phi_V, \Delta\phi(\alpha)), \quad (6)$$

where $\Delta\phi_V$ is associated to the vortex shedding mechanism, while $\Delta\phi(\alpha)$ is associated to the gaseous fuel oscillations. Since the pilot flame strongly depends on the fuel split α , but not the multi-point flame (Fig. 12), the comparison between $\Delta\phi_Q$ and $\Delta\phi$ will give access to which mechanism is affecting the system: (1) if $\Delta\phi_Q$ also depends strongly on the fuel split α , like $\Delta\phi$ does, then the gaseous fuel oscillation at the pilot zone is controlling the instabilities ; (2) Otherwise $\Delta\phi_Q$ does not depend on the fuel split α , which implies that vortex shedding at the multi-point zone is dominating. To do so, for the three fuel split values, the global (pilot+multi-point zones) unsteady heat release $q'(t)$ is correlated to the acoustic pressure $p'(t)$ to determine $\Delta\phi_Q$.

Figure 17 shows the filtered heat release and pressure fluctuations for several fuel split parameters: $\alpha = 5\%$, 10% , and 20% . The global unsteady combustion is correlated directly to pressure oscillations giving a constant phase-lag here (Fig. 18, right): for all fuel split parameters, $\Delta\phi_Q/2\pi \approx 0.41 - 0.46$ for $f = 1.0$ and $\Delta\phi_Q/2\pi \approx 0.64 - 0.67$ for $f = 1.84$. Consequently, the phase-lag of the whole system is almost insensitive to the fuel staging α (Fig. 18, right). It suggests that vortex shedding in the multi-point zone is the key mechanism leading to combustion instabilities, whereas the pilot flame has only a marginal effect in the present case. Nevertheless, this second mechanism, proved to change drastically with the fuel split α ($\Delta\phi$ in Fig. 18, left), could impact other key features of the engine such as pollutant emissions and temperature profiles at the turbine inlet. Moreover, fuel oscillations in the pilot zone may have a significant role in other operating conditions, like the idle regime where most of the power is supplied by the pilot flames ($\alpha \approx 100\%$).

CONCLUSION

This paper describes the application of a coupled approach LES/Acoustic model to assess the effect of fuel split on combustion instabilities in an industrial ultra low-NOx annular combustor. Multiphase flow LES and an analytical model (ATACA-

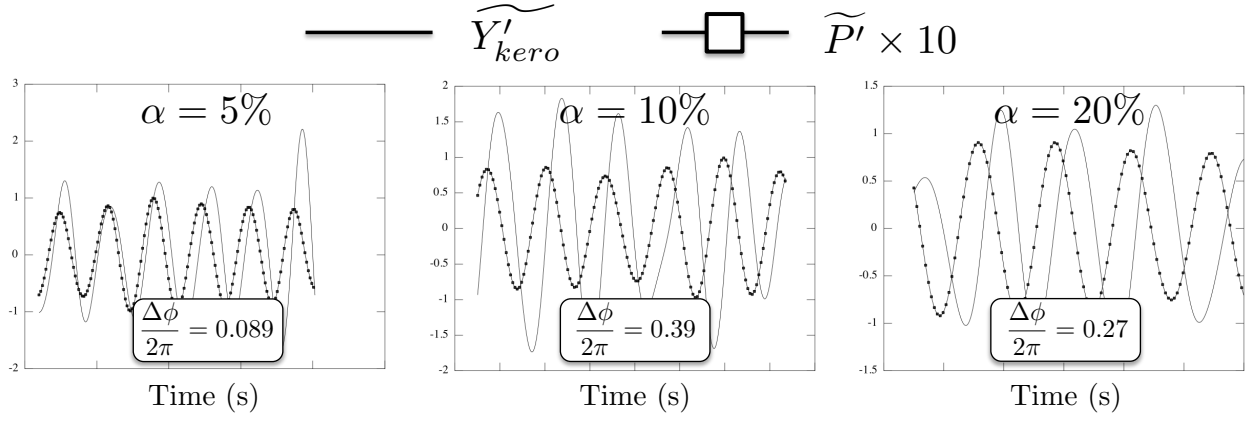


FIGURE 16: Normalized relative pressure \tilde{P}' and fuel mass fractions \tilde{Y}'_{kero} oscillations for the case at $f = 1.84$ and fuel splits $\alpha = 5\%$ (left) $\alpha = 10\%$ (middle) and $\alpha = 20\%$ (right). Normalized phase lags $\Delta\phi/2\pi$ between fuel and pressure oscillations are extracted.

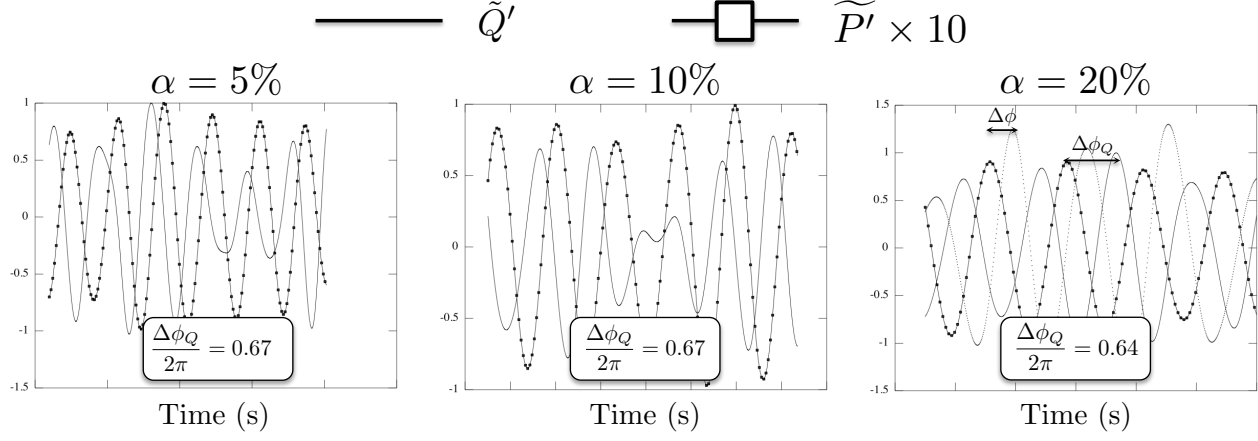


FIGURE 17: Normalized relative pressure \tilde{P}' and heat release \tilde{Q}' oscillations for the case at $f = 1.84$ and fuel splits $\alpha = 5\%$ (left) $\alpha = 10\%$ (middle) and $\alpha = 20\%$ (right). Normalized phase lags $\Delta\phi_Q/2\pi$ between heat release and pressure oscillations are also displayed. The fuel oscillations and associated phase lag $\Delta\phi/2\pi$ are shown for the case $\alpha = 20\%$ (right).

MAC) for thermoacoustic modes are combined to provide characteristic phase-lags of two mechanisms leading to thermoacoustic instabilities: (1) acoustics generates vortex shedding, which can interact with the flame and (2) acoustics can modify the liquid/gaseous fuel transport and the evaporation process leading to gaseous fuel oscillations. The aim of this paper is to identify and then investigate these two mechanisms by changing the fuel split (mainly affecting mechanism 2 in the pilot zone) and therefore assess which mechanism controls the flame dynamics. First, the eigenmodes of the annular chamber are investigated using the analytical model ATACAMAC and validated by 3D Helmholtz simulations. Then, multiphase flow LES are forced at the eigenfrequencies of the chamber for three different fuel split values. From the authors knowledge, acoustically forcing a multiphase flow LES was never done before and constitutes the main goal

of this paper. In particular, a specific method called LADTF (Locally Adaptative Dynamic Thickened Flames model) is described to handle the complex combustion process occurring in such systems containing multi-point injection devices. Key features of the flow and flame response to acoustics are investigated. The characteristic phase-lags associated with these two mechanisms are extracted. Results show that acoustic forcing generates gaseous oscillations in the pilot zone, which strongly depend on the fuel split parameter. However, the correlation between the global heat release fluctuations and acoustics highlights no dependency with the fuel split parameter. Therefore, it suggests that Mechanism 1, associated to vortex shedding in the multi-point zone and almost not depending on the fuel split, is the main feature controlling the flame dynamics in the LEMCOTEC engine. It also proves that acoustically forced multiphase flow LES

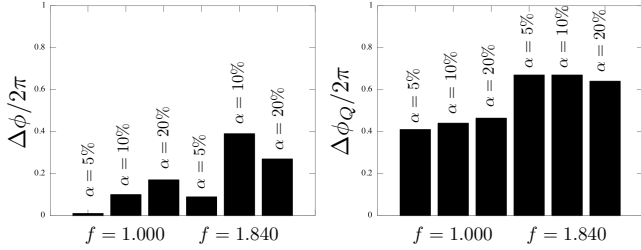


FIGURE 18: Phase lags associated to the gaseous fuel oscillations ($\Delta\phi$, left) and global phase-lag corresponding to the acoustics/unsteady combustion interactions ($\Delta\phi_Q$, right) for cases forced at $f = 1.0$ and 1.84 and fuel split parameters $\alpha = 5\%$, 10% and 20% .

is a suitable approach to analyze underlying multiphase flow phenomena leading to combustion instabilities in complex industrial annular combustors. Even though the fuel split does not affect combustion instabilities here, other operating conditions where power is mostly supplied by the pilot flame may be influenced by the fuel staging. Moreover, fuel split can also impact pollutant emissions or temperature profiles at the turbine inlet, issues still under investigation today.

ACKNOWLEDGMENTS

This work is financially supported by the European Commission under the “LEMCOTEC - Low Emissions Core-Engine Technologies”, a Collaborative Project co-funded by the European Commission within the Seventh Framework Programme (2007-2013) under the Grant Agreement n° 283216. Simulations presented in this paper have been performed using HPC resources provided by GENCI [TGCC/CINES/IDRIS] on the supercomputer CURIE.

REFERENCES

- [1] Poinsot, T., Trouvé, A., Veynante, D., Candel, S., and Esposito, E., 1987. “Vortex driven acoustically coupled combustion instabilities”. *J. Fluid Mech.*, **177**, pp. 265–292.
- [2] Paschereit, C. O., and Gutmark, E., 1999. “Control of thermoacoustic instabilities in a premixed combustor by fuel modulation”. In 37th AIAA Aerospace Sciences Meeting and Exhibit, A. P. 99-0711, ed.
- [3] Lieuwen, T., and Yang, V., 2005. *Combustion Instabilities in Gas Turbine Engines. Operational Experience, Fundamental Mechanisms and Modeling*. Progress in Astronautics and Aeronautics, AIAA.
- [4] Krebs, W., Flohr, P., Prade, B., and Hoffmann, S., 2002. “Thermoacoustic stability chart for high intense gas turbine combustion systems”. *Combust. Sci. Tech.*, **174**, pp. 99–128.
- [5] Worth, N., and Dawson, J., 2013. “Self-excited circumferential instabilities in a model annular gas turbine combustor: global flame dynamics”. In *Proc. Combust. Inst.*, Vol. 34, pp. 3127–3134.
- [6] Noiray, N., Bothien, M., and Schuermans, B., 2011. “Investigation of azimuthal staging concepts in annular gas turbines”. *Combust. Theory and Modelling*, pp. 585–606.
- [7] Stow, S. R., and Dowling, A. P., 2001. “Thermoacoustic oscillations in an annular combustor”. In ASME Paper, no. 2001-GT-0037.
- [8] Parmentier, J., Salas, P., Wolf, P., Staffelbach, G., Nicoud, F., and Poinsot, T., 2012. “A simple analytical model to study and control azimuthal instabilities in annular combustion chamber”. *Combustion and Flame*, **159**, pp. 2374–2387.
- [9] Ghirardo, G., and Juniper, M., 2013. “Azimuthal instabilities in annular combustors: standing and spinning modes”. In *Proceedings of the Royal Society A*, no. 2013-0232.
- [10] Campa, G., and Camporeale, S., 2014. “Prediction of thermoacoustic combustion instabilities in practical annular combustors”. *J. Eng. Gas Turbines Power*, **136**(9).
- [11] Pankiewitz, C., and Sattelmayer, T., 2003. “Time domain simulation of combustion instabilities in annular combustors”. *ASME Journal of Engineering for Gas Turbines and Power*, **125**(3), pp. 677–685.
- [12] Wolf, P., Staffelbach, G., Gicquel, L., Muller, J., and T., P., 2012. “Acoustic and large eddy simulation studies of azimuthal modes in annular combustion chambers”. *Combustion and Flame*, **159**, pp. 3398–3413.
- [13] Bauerheim, M., 2014. “Theoretical and numerical study of symmetry breaking effects on azimuthal thermoacoustic modes in annular combustors”. PhD thesis, CERFACS and INP Toulouse, 1st December.
- [14] Bauerheim, M., Staffelbach, G., Worth, N., Dawson, J., Gicquel, L., and Poinsot, T., 2015. “Sensitivity of least-based harmonic flame response model for turbulent swirled flames and impact on the stability of azimuthal modes”. *Proc. Combust. Inst.*, **35**(3), pp. 3355–3363.
- [15] Lieuwen, T., and Zinn, B. T., 1998. “The role of equivalence ratio oscillations in driving combustion instabilities in low nox gas turbines”. *Proc. Combust. Inst.*, **27**, pp. 1809–1816.
- [16] Lovett, J., 1995. Multi-stage fuel nozzle for reducing combustion instabilities in low nox gas turbines, Apr. 25. US Patent 5,408,830.
- [17] Nicoud, F., Benoit, L., Sensiau, C., and Poinsot, T., 2007. “Acoustic modes in combustors with complex impedances and multidimensional active flames”. *AIAA Journal*, **45**, pp. 426–441.
- [18] Bauerheim, M., Parmentier, J., Salas, P., Nicoud, F., and

- Poinsot, T., 2014. "An analytical model for azimuthal thermoacoustic modes in an annular chamber fed by an annular plenum". *Combustion and Flame*, **161**, pp. 1374–1389.
- [19] Evesque, S., Polifke, W., and Pankiewitz, C., 2003. "Spinning and azimuthally standing acoustic modes in annular combustors". In 9th AIAA/CEAS Aeroacoustics Conference, Vol. AIAA paper 2003-3182.
- [20] Bauerheim, M., Cazalens, M., and Poinsot, T., 2015. "A theoretical study of mean azimuthal flow and asymmetry effects on thermo-acoustic modes in annular combustors". *Proc. Combust. Inst.*, **35**(3), pp. 3219–3227.
- [21] Bauerheim, M., Salas, P., Nicoud, F., and Poinsot, T., 2014. "Symmetry breaking of azimuthal thermoacoustic modes in annular cavities: a theoretical study". *J. Fluid Mech.*, **760**, pp. 431–465.
- [22] Cazalens, M., Esclapez, L., Bauerheim, M., Jaravel, T., Riber, E., Cuenot, B., Poinsot, T., Voivenel, L., and Danaila, L., 2014. "Development of ultra lean combustion systems for high opr systems". In 3AF CleanSky Conference.
- [23] Poinsot, T., and Veynante, D., 2011. *Theoretical and Numerical Combustion*. Third Edition (www.cerfacs.fr/elearning).
- [24] Lacaze, G., Richardson, E., and Poinsot, T. J., 2009. "Large eddy simulation of spark ignition in a turbulent methane jet". *Combust. Flame*, **156**(6), pp. 1993–2009.
- [25] Kuenne, G., Ketelheun, A., and Janicka, J., 2011. "LES modeling of premixed combustion using a thickened flame approach coupled with fgm tabulated chemistry". *Combust. Flame*, **158**(9), pp. 1750 – 1767.
- [26] Colin, O., Ducros, F., Veynante, D., and Poinsot, T., 2000. "A thickened flame model for large eddy simulations of turbulent premixed combustion". *Phys. Fluids*, **12**(7), pp. 1843–1863.
- [27] Nicoud, F., and Poinsot, T., 1999. "Dns of a channel flow with variable properties". In Int. Symp. On Turbulence and Shear Flow Phenomena.
- [28] Poinsot, T., and Lele, S., 1992. "Boundary conditions for direct simulations of compressible viscous flows". *J. Comput. Phys.*, **101**(1), pp. 104–129.
- [29] Jaegle, F., 2009. "Les of two-phase flow in aero-engines". PhD thesis, Université de Toulouse - Ecole doctorale MEGeP, CERFACS - CFD Team, Toulouse, December.
- [30] Becker, J., and Hassa, C., 2002. "Breakup and atomization of a kerosene jet in crossflow at elevated pressure". *Atomization and Sprays*, **12**(1-3), pp. 49–68.
- [31] Lavedrine, J., 2008. "Simulations aux grandes échelles de l'écoulement diphasique dans des modèles d'injecteur de moteurs aéronautiques". Phd thesis, INP Toulouse.
- [32] Bertier, N., Dupoirieux, F., Mtuszewski, L., and Guin, C., 2008. "Simulation numérique d'une chambre de combustion multipoint". In 2nd colloque INCA.
- [33] Boileau, M., Staffelbach, G., Cuenot, B., Poinsot, T., and Bérat, C., 2008. "LES of an ignition sequence in a gas turbine engine". *Combust. Flame*, **154**(1-2), pp. 2–22.
- [34] Sanjosé, M., Lederlin, T., Gicquel, L., Cuenot, B., Pitsch, H., García-Rosa, N., Lecourt, R., and Poinsot, T., 2008. "Les of two-phase reacting flows". In Proceedings of the Summer Program 2008, CTR, ed., pp. 251–263.
- [35] Charlette, F., Veynante, D., and Meneveau, C., 2002. "A power-law wrinkling model for LES of premixed turbulent combustion: Part I - non-dynamic formulation and initial tests". *Combust. Flame*, **131**, pp. 159–180.
- [36] Blimbaum, J., Zanchetta, M., Akin, T., Acharya, V., J.O'Connor, Noble, D., and Lieuwen, T., 2012. "Transverse to longitudinal acoustic coupling processes in annular combustion chambers". *International journal of spray and combustion dynamics*, **4**(4), pp. 275–298.
- [37] Jangi, M., and Kobayashi, H., 2009. "Heat and mass transfer of a fuel droplet evaporating in oscillatory flow". *International Journal of Heat and Fluid Flow*, **30**(4), pp. 729–740.